Integrated Sensing and Communications With Mixed Fields Using Transmit Beamforming

Yun Xiao, Enhao Wang, Yunfei Chen, *Senior Member, IEEE,* Li Chen, *Senior Member, IEEE,* Aissa Ikhlef, *Senior Member, IEEE,* and Hongjian Sun, *Senior Member, IEEE*

***Abstract*—Integrated sensing and communications (ISAC) is an important enabling technology for the next-generation wireless systems. Owing to the use of large-scale antenna arrays and/or high carrier frequencies, the communications user and the target may follow different propagation models. However, most existing works assume either far-field or near-field propagation models for both communications and sensing. In this work, a realistic case is considered when the communications user and the target are in different fields. New beamforming designs are proposed to optimize the sensing performance considering a bi-static setting. Specifically, the sensing signal-to-clutter-plus-noise ratio (SCNR) is optimized, and a generalized iterative algorithm is proposed to solve the optimization problem. Numerical results show the effects of model mismatch between near-field and far-field, antenna size and communications channel on the sensing performance.**

***Index Terms*—Beamforming, bi-static sensing, far-filed, integrated sensing and communications, model mismatch, near-field.**

I. Introduction

In integrated sensing and communications (ISAC), the sensing and communications functions are integrated in the same hardware platform, enabling efficient utilization of shared spectrum resources [1]. On the other hand, 6G is expected to employ extremely large-scale antenna arrays (XL-array), high frequencies (e.g. millimeter wave and terahertz), and new types of antennas to increase data rates [2]. This makes the range of the near-field (NF) region or the effective Rayleigh distance, which is a threshold not the actual communication distance, considerable [2]. Unlike the far-field (FF) plane wave model that focuses the beam at a specific direction, the NF spherical wave model focuses the beam at a specific location, bringing new challenges to ISAC designs [3].

Beamforming (BF) is widely used in ISAC to guarantee the performances of sensing or communications. In [4], the BF vectors were optimized for sensing-centric and communication-centric scenarios. In [5], Cramér-Rao bound (CRB) for parameter estimation was considered as a sensing performance metric, while ensuring the signal-to-interference-plus-noise ratio (SINR) and sum rate of the communications users (CUs), respectively. The bi-static and multi-static sensing models were considered in [6] and [7], respectively. The aforementioned studies have considered only the FF plane wave model. Recently, due to the use of large-scale antenna arrays and high carrier frequencies, the BF design for NF ISAC has also attracted a lot of attention [8], [9].

All these works assume that the CU and the target follow the same propagation model. However, in practice, due to different locations of the CU and the target, it is possible that the CU and the target may follow different propagation models so that mixed FF and NF scenario needs to be considered for ISAC. Reference [10] considered mixed FF and NF scenarios for massive multiple-input-multiple-output (MIMO) systems, but without sensing. The main challenges in this scenario include the model mismatch between FF and NF, which could cause performance loss [11], and the increased design complexity [10]. References [4] to [7] used randomly generated channels for CUs and fixed channel gains for targets assuming the same fields. Thus, a mixed-field ISAC design is needed.

Motivated by the above observations, this work explores mixed-field ISAC in a bi-static setting with separate transmitter (Tx) and receiver (Rx). Two specific scenarios are studied: FF communications with NF target (NFS-FFC) and NF communications with FF target (FFS-NFC). Transmit BF is performed to optimize the sensing SCNR while meeting constraints on communications SINR and transmit power. Numerical results quantify the performance loss of the mixed ISAC system caused by the model mismatch. They also show that the sensing performance improves with the decrease of communications' SINR or rate requirements and the increase of antenna size.

II. System Model

As shown in Fig. 1, an ISAC system simultaneously communicates with multiple CUs and detects a target. The dual-functional base station (BS) has N_t transmit antennas and serves K single-antenna CUs denoted by $k \in \{1, ..., K\}$. The bi-static sensing receiver with N_r receive antennas receives the echo signal from the target. Suppose that L is the total number of samples during which the CUs and the target are approximately static. The data signal transmitted by the BS is

$$\mathbf{s}\left[l\right] = \sum_{k=1}^{K} \mathbf{b}_k d_k\left[l\right], l = 1, \ldots, L, \tag{1}$$

This work was supported in part by the King Abdullah University of Science and Technology Research Funding (KRF) under Award ORA-2021-CRG10-4696 and by EPSRC TITAN (EP/Y037243/1, EP/X04047X/1).

Yun Xiao, Enhao Wang, Yunfei Chen, Aissa Ikhlef, and Hongjian Sun are with the Department of Engineering, Durham University, Durham DH1 3LE, United Kingdom (e-mail: yun.xiao, enhao.wang, yunfei.chen, aissa.ikhlef, hongjian.sun@durham.ac.uk).

Li Chen is with the CAS Key Laboratory of Wireless-Optical Communications, University of Science and Technology of China, Hefei 230027, China (e-mail:chenli87@ustc.edu.cn).

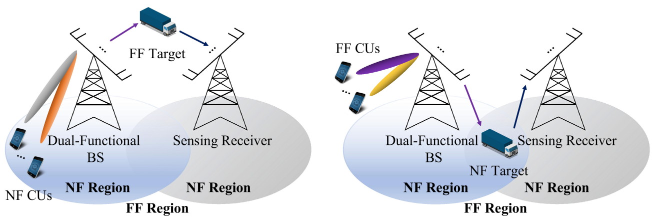

(a) FFS-NFC (b) NFS-FFC

Fig. 1: Bistatic ISAC system model.

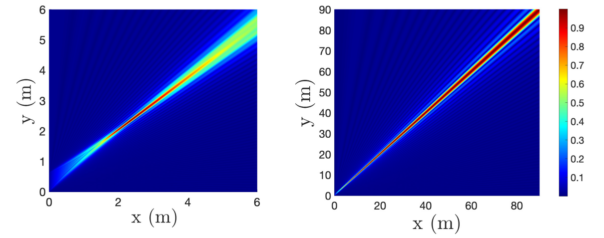

(a) NF (b) FF

Fig. 2: Normalized beamforming gain for a ULA BS with 129 antennas operating at 30 GHz.

where $\mathbf{b}_k \in \mathcal{C}^{N_t\times 1}$ and $d_k[l] \in \mathcal{C}$ are the transmit beamforming vector and data sample of the k-th CU, respectively. The data samples are assumed to be Gaussian distributed with $d_k[l] \sim \mathcal{CN}(0,1)$. Thus, $\mathbf{s}[l] \in \mathcal{C}^{N_t\times 1}$ contains data signals for all CUs. Given the maximum transmit power P_0, the power constraint of the BS can be expressed as

$$\mathrm{E}(\|\mathbf{s}[l]\|^2) = \sum_{k=1}^{K} \mathrm{tr}(\mathbf{b}_k\mathbf{b}_k^H) \le P_0. \tag{2}$$

A. Channel Model

We adopt the effective Rayleigh distance as the NF range metric [2]. The division between the NF and FF regions depends on whether the distance from the BS is less than or greater than the effective Rayleigh distance, denoted by $d_{F(eff)} = \left(0.367\sin^2\theta\right)\frac{2D^2}{\lambda}$, where D is the antenna aperture, θ is the target angle, and λ is the wavelength of the carrier frequency [2]. We assume that the BS uses a uniform linear array (ULA), and that the distance between adjacent antennas at the BS is $d = \frac{\lambda}{2}$.

*1) **Near-field channel model**:* Suppose that the origin of the coordinate system is set at the center of the BS. The coordinate of the user or target is $R = [r_{NF}\sin(\theta), r_{NF}\cos(\theta)]$, where r_{NF} is the distance from the origin when the user or target is located in the NF region with $r_{NF} < d_{F(eff)}$, and $\theta \in [\frac{-\pi}{2}, \frac{\pi}{2}]$ is the angle between the y-axis and the user or target. The coordinate of the n-th antenna is denoted as $[\delta^{(n)}d, 0]$, where $n \in [0,\dots,N_t-1]$ and $\delta^{(n)} = n - \frac{N_t-1}{2}$. According to the cosine theorem for trigonometric functions, the distance between the n-th antenna and the user or target can be calculated as $r^{(n)} = \sqrt{r_{NF}^2 + \left(\delta^{(n)}d\right)^2 - 2r_{NF}\delta^{(n)}d\sin(\theta)}$. The NF channel at the n-th antenna can be modeled as $h_{near}^{(n)} = \tilde{\beta}_{near}^{(n)} e^{-j\frac{2\pi}{\lambda}r^{(n)}} = \beta_{near}^{(n)} e^{-j\frac{2\pi}{\lambda}\left(r^{(n)}-r_{NF}\right)}$ [12], where $\beta_{near}^{(n)} = \frac{\rho_0}{r^{(n)}} e^{-j\frac{2\pi}{\lambda}r_{NF}}$ is the complex channel gain, and $\rho_0 = \frac{\lambda}{4\pi}$ is the reference free-space path gain at a distance of 1 m [13]. In the Fresnel region, assume that $\beta_{near}^{(0)} \approx \cdots \approx \beta_{near}^{(\frac{N_t-1}{2})} = \beta_{near} = \frac{\rho_0}{r_{NF}} e^{-j\frac{2\pi}{\lambda}r_{NF}}$ when $r_{NF} > D$ [12]. As such, the NF channel vector can be modeled as

$$\mathbf{h}_{near} = \beta_{near}\mathbf{a}\left(r_{NF},\theta\right), \tag{3}$$

where $\mathbf{a}\left(r_{NF},\theta\right)$ is the NF beam focusing vector with $\mathbf{a}\left(r_{NF},\theta\right) = \left[e^{-j\frac{2\pi}{\lambda}\left(r^{(0)}-r_{NF}\right)},\dots,e^{-j\frac{2\pi}{\lambda}\left(r^{(n)}-r_{NF}\right)}\right]^T$. As shown in Fig. 2(a), both the distance r_{NF} and the angle θ determine the energy of NF beam.

*2) **Far-field channel model**:* When the user or target is located in the FF region at a distance of $r_{FF} > d_{F(eff)}$ and an angle of φ from the center of ULA, the NF beam focusing vector becomes the FF beam steering vector. By applying the first-order Taylor expansion $\sqrt{1+\mu} \approx 1 + \frac{1}{2}\mu$ to $r^{(n)}$, one has $r^{(n)} \approx \hat{r}^{(n)} = r_{FF} - \delta^{(n)}d\sin(\varphi)$ [8]. Similar to the NF channel, the FF channel can be expressed as

$$\mathbf{h}_{far} = \beta_{far}\mathbf{a}(\varphi), \tag{4}$$

where $\beta_{far} = \frac{\rho_0}{r_{FF}} e^{-j\frac{2\pi}{\lambda}r_{FF}}$ is the complex-valued channel gain, and $\mathbf{a}(\varphi)$ is the FF beam steering vector with $\mathbf{a}(\varphi) = [e^{j\frac{2\pi d}{\lambda}(\delta^{(0)})\sin(\varphi)},\dots,e^{j\frac{2\pi d}{\lambda}(\delta^{(n)})\sin(\varphi)}]^T$. As shown in Fig. 2(b), when the distance is greater than $d_{F(eff)}$, only the angle φ of the target or user determines the beam energy. Note that in practice, an initial training period can determine the propagation model using the mixed localization and the exact model (MILE) method [11]. Sensing parameters can be determined by methods like maximum likelihood estimation (MLE) [14]. For example, in [8] - [10], the channel models and channel gains were assumed known before beamforming. In [4] - [7], the locations of communications users and the target were assumed different but known as well. Similar to these previous works that assume known far-field or near-field, this work assumes known mixed-field, but the model estimation is beyond the scope of the work.

B. Communications Model

Using the transmitted signal $\mathbf{s}[l]$ in (1), the received signal at the k-th CU is given by

$$y_k[l] = \mathbf{h}_k^T\mathbf{b}_k d_k[l] + \sum_{i\ne k}\mathbf{h}_k^T\mathbf{b}_i d_i[l] + z_k[l], \tag{5}$$

where $\mathbf{h}_k \in \{(\mathbf{h}_{near})_k \text{ or } (\mathbf{h}_{far})_k\}$ is the $N_t \times 1$ channel vector of the k-th CU, $z_k[l] \sim \mathcal{CN}(0,\mathbf{I})$ is the additive white Gaussian noise (AWGN) at user k. Then the received SINR at the k-th CU can be expressed as

$$\gamma_k = \frac{\left|\mathbf{h}_k^T\mathbf{b}_k\right|^2}{\sum\limits_{i=1,i\ne k}^{K}\left|\mathbf{h}_k^T\mathbf{b}_i\right|^2 + 1} = \frac{\mathbf{h}_k^T\mathbf{b}_k\mathbf{b}_k^H\mathbf{h}_k^*}{\sum\limits_{i=1,i\ne k}^{K}\mathbf{h}_k^T\mathbf{b}_i\mathbf{b}_i^H\mathbf{h}_k^* + 1}. \tag{6}$$

C. Sensing Model

Using the transmitted signal $\mathbf{s}[l]$ in (1), the received signal at the sensing receiver can be expressed as

$$\begin{aligned}\mathbf{y}[l] &= \beta_s \mathbf{a}_r \mathbf{a}_t^T \mathbf{s}[l] + \textstyle\sum_{j=1}^{C} \beta_j \mathbf{a}_{rj} \mathbf{a}_{tj}^T \mathbf{s}[l] + \mathbf{z}_s[l] \\ &= \beta_s \mathbf{A}\mathbf{s}[l] + \textstyle\sum_{j=1}^{C} \beta_j \mathbf{A}_j \mathbf{s}[l] + \mathbf{z}_s[l],\end{aligned} \tag{7}$$

where $\sum_{j=1}^{C}\beta_j \mathbf{A}_j \mathbf{s}[l]$ is the clutter signal, C is the number of clutters, $\mathbf{z}_s[l] \sim \mathcal{CN}(0,\mathbf{I})$ is the AWGN, $\beta_s, \beta_j = \frac{\rho_0}{r_t+r_r} e^{-j\frac{2\pi}{\lambda}(r_t+r_r)}\sigma$ are the complex channel gains, where r_t and r_r are the distances of the target or clutter from the Tx and Rx, respectively, and σ is the reflection coefficient of the target or clutter. Assume that the clutter and target are located in the same field. Also, $\mathbf{a}_r$, $\mathbf{a}_{rj}$ and $\mathbf{a}_t$, $\mathbf{a}_{tj}$ denote the beam steering or focusing vectors of receive BS and transmit BS, respectively, and $\mathbf{A}, \mathbf{A}_j \in \mathcal{C}^{N_r \times N_t}$ are the beam steering or focusing matrices. Then the output of the sensing receiver is

$$r[l] = \mathbf{f}^H \mathbf{y}[l] = \beta_s \mathbf{f}^H \mathbf{A}\mathbf{s}[l] + \mathbf{f}^H \textstyle\sum_{j=1}^{C} \beta_j \mathbf{A}_j \mathbf{s}[l] + \mathbf{f}^H \mathbf{z}_s[l], \tag{8}$$

where $\mathbf{f} \in \mathcal{C}^{N_r \times 1}$ is the receive beamforming vector. The SCNR is given by [1]

$$\begin{aligned}\gamma_s &= \mathrm{E}\left[\frac{\left|\beta_s \mathbf{f}^H \mathbf{A}\mathbf{s}[l]\right|^2}{\mathbf{f}^H\left(\sum_{j=1}^{C}|\beta_j|^2 \mathbf{A}_j \mathbf{s}[l]\mathbf{s}[l]^H \mathbf{A}_j^H + \mathbf{I}\right)\mathbf{f}}\right] \\ &= \frac{|\beta_s|^2\left(\sum_{k=1}^{K}\mathbf{f}^H \mathbf{A}\mathbf{b}_k \mathbf{b}_k^H \mathbf{A}^H \mathbf{f}\right)}{\mathbf{f}^H\left(\sum_{j=1}^{C}\sum_{k=1}^{K}|\beta_j|^2 \mathbf{A}_j \mathbf{b}_k \mathbf{b}_k^H \mathbf{A}_j^H + \mathbf{I}\right)\mathbf{f}}.\end{aligned} \tag{9}$$

To maximize the SCNR, the optimal $\mathbf{f}$ is [4]

$$\mathbf{f}_{opt} = \textstyle\sum_{k=1}^{K} \alpha (\mathbf{R}_c + \mathbf{I})^{-1} \mathbf{A}\mathbf{b}_k, \tag{10}$$

where $\mathbf{R}_c = \sum_{j=1}^{C}\sum_{k=1}^{K}|\beta_j|^2 \mathbf{A}_j \mathbf{b}_k \mathbf{b}_k^H \mathbf{A}_j^H$ is the covariance matrix of the clutters, α is an arbitrary constant that can be derived by solving the minimum variance distortionless response (MVDR) problem [4] to give

$$\mathbf{f}_{opt} = \frac{\sum_{k=1}^{K}(\mathbf{R}_c + \mathbf{I})^{-1}\mathbf{A}\mathbf{b}_k}{\sum_{k=1}^{K}\mathbf{b}_k^H \mathbf{A}^H (\mathbf{R}_c + \mathbf{I})^{-1}\mathbf{A}\mathbf{b}_k}. \tag{11}$$

By substituting (11) into (9), the SCNR of sensing is

$$\gamma_s = \sum_{k=1}^{K} \mathrm{tr}\left(|\beta_s|^2 \mathbf{b}_k^H \mathbf{A}^H (\mathbf{R}_c + \mathbf{I})^{-1} \mathbf{A}\mathbf{b}_k\right) = \sum_{k=1}^{K} \mathrm{tr}(\Psi \mathbf{b}_k \mathbf{b}_k^H), \tag{12}$$

where $\Psi = |\beta_s|^2 \mathbf{A}^H (\mathbf{R}_c + \mathbf{I})^{-1} \mathbf{A}$.

III. Beamforming Design

We aim to maximize the sensing SCNR under the constraints of the SINR of CUs and BS transmit power, which can be formulated as

$$\begin{aligned}(\mathrm{P1})\ \max_{\{\mathbf{b}_k\}}\ & \sum_{k=1}^{K} \mathrm{tr}\left(\Psi \mathbf{b}_k \mathbf{b}_k^H\right) && (13\mathrm{a}) \\ \text{s.t.}\ & \sum_{k=1}^{K} \mathrm{tr}(\mathbf{b}_k \mathbf{b}_k^H) \le P_0 && (13\mathrm{b}) \\ & \frac{\mathbf{h}_k^T \mathbf{b}_k \mathbf{b}_k^H \mathbf{h}_k^*}{\sum_{i=1, i\neq k}^{K} \mathbf{h}_k^T \mathbf{b}_i \mathbf{b}_i^H \mathbf{h}_k^* + 1} \ge \Gamma_k, \forall k, && (13\mathrm{c})\end{aligned}$$

where Γ_k is the SINR constraint of the k-th CU. (13c) is equivalent to a per user rate constraint from (6). Problem (P1) is non-convex due to the quadratic objective (13a), the quadratic constraint (13b), and the quadratic fractional constraint (13c). To make it convex, the semidefinite relaxation (SDR) method in [15] is used to relax the quadratic objective and quadratic constraints by letting $\mathbf{B}_k = \mathbf{b}_k \mathbf{b}_k^H$, where $\mathbf{B}_k$ is the covariance matrix of the k-th CU with $\mathbf{B}_k \succeq 0$ and $\mathrm{rank}(\mathbf{B}_k) = 1$. This remains non-convex due to the rank-one constraint. Thus, it is dropped to reformulate the problem as

$$\begin{aligned}(\mathrm{P1.1})\ \max_{\{\mathbf{B}_k\}}\ & \sum_{k=1}^{K} \mathrm{tr}\left(\hat{\Psi} \mathbf{B}_k\right) && (14\mathrm{a}) \\ \text{s.t.}\ & \sum_{k=1}^{K} \mathrm{tr}(\mathbf{B}_k) \le P_0 && (14\mathrm{b}) \\ & \frac{\mathbf{h}_k^T \mathbf{B}_k \mathbf{h}_k^*}{\Gamma_k} - \sum_{i=1, i\neq k}^{K} \mathbf{B}_i \mathbf{h}_k^* \mathbf{h}_k^T - 1 \ge 0, \forall k && (14\mathrm{c}) \\ & \mathbf{B}_k \succeq 0, \forall k. && (14\mathrm{d})\end{aligned}$$

We propose an iterative algorithm to solve it, which is shown in Algorithm 1. $\hat{\Psi}$ is defined in Algorithm 1. In each iteration, $\hat{\Psi}$ is regarded as a constant and calculated using $\{\mathbf{B}_k\}$ optimized from the previous iteration. Assuming that the number of iterations is M, the complexity can be derived as $\mathcal{O}\left(M\left(KN_t^2\right)^3\right)$. Problem (P1.1) is a semi-definite programming (SDP) problem, so it can be solved by CVX [16]. After deriving the optimized $\{\mathbf{B}_k\}$ from (14) in the last iteration, the solution to (13) can be calculated and approximated as [8]

$$\mathbf{b}_k^\dagger = \left(\mathbf{h}_k^T \mathbf{B}_k \mathbf{h}_k^*\right)^{-\frac{1}{2}} \mathbf{B}_k \mathbf{h}_k^*, \forall k. \tag{15}$$

Algorithm 1 Proposed Iterative Algorithm for BF Design

1: Initialize the convergence precision δ_γ, and the number of iterations $ite = 0$.
2: Initialize the objective variables $\left\{\mathbf{B}_k^{(0)} = \mathbf{I}\right\}$.
3: **repeat**
4: Update $ite = ite + 1$.
5: Calculate the sensing SCNR $\gamma_s^{(ite-1)}$ and $\hat{\Psi}$ based on $\{\mathbf{B}_k\}^{(ite-1)}$ according to (12).
6: Optimize $\{\mathbf{B}_k\}^{(ite)}$ according to the problem in (14).
7: **until** $\left|\gamma_s^{(ite)} - \gamma_s^{(ite-1)}\right| \le \delta_\gamma$
8: Calculate $\left\{\mathbf{b}_k^\dagger\right\}$ by (15).

The optimized SCNR is upper-bounded, and monotonically non-decreasing with the number of iterations and hence the algorithm converges. For the NF sensing and FF communications (NFS-FFC) scenario, $(\mathrm{P1.1})$ is specialized to

$$(\mathrm{P2}) \max_{\{\mathbf{B}_k\}} \sum_{k=1}^{K} \operatorname{tr}\left(\hat{\Psi}_{near}\mathbf{B}_k\right) \tag{16a}$$

$$\text{s.t.} \quad \frac{(\mathbf{h}_{far})_k^T \mathbf{B}_k (\mathbf{h}_{far})_k^*}{\Gamma_k} - \sum_{i \neq k}^{K} \mathbf{B}_i (\mathbf{h}_{far})_k^* (\mathbf{h}_{far})_k^T - 1 \geq 0, \forall k, (14\mathrm{b}), \text{and} (14\mathrm{d}), \tag{16b}$$

where $\hat{\Psi}_{near}$ from (12) contains NF beam focusing matrices and channel gains of the target and the clutters. For the FF sensing and NF communications (FFS-NFC) scenario, $(\mathrm{P1.1})$ becomes

$$(\mathrm{P3}) \max_{\{\mathbf{B}_k\}} \sum_{k=1}^{K} \operatorname{tr}\left(\hat{\Psi}_{far}\mathbf{B}_k\right) \tag{17a}$$

$$\text{s.t.} \quad \frac{(\mathbf{h}_{near})_k^T \mathbf{B}_k (\mathbf{h}_{near})_k^*}{\Gamma_k} - \sum_{i \neq k}^{K} \mathbf{B}_i (\mathbf{h}_{near})_k^* (\mathbf{h}_{near})_k^T - 1 \geq 0, \forall k, (14\mathrm{b}), \text{and} (14\mathrm{d}), \tag{17b}$$

where $\hat{\Psi}_{far}$ from (12) contains FF beam steering matrices and channel gains of the target and the clutters. Both $(\mathrm{P2})$ and $(\mathrm{P3})$ are solved using Algorithm 1 with relevant parameters.

IV. Numerical Results And Discussion

Next, numerical results are given. Tx and Rx are located at $(0,0)$ and $(d_{F(eff)},0)$, respectively. The system operates at 30 GHz with $N_t = N_r = 129$ and $d = \frac{\lambda}{2}$, which gives $d_{F(eff)} = 15.03$ m. The transmit power and noise power are set to 30 dBm and -70 dBm, respectively. There are 4 CUs and one target in both scenarios. The distances of NF CUs or target from the Tx are set to 10 m, and the distances of FF CUs or target from the Tx are set to 35 m. The transmit angles of CUs and target are set to $\{-45°, -30°, -15°, 0°\}$ and $45°$, respectively. The coordinate of the target with respect to the sensing receiver can be calculated from the cosine theorem. Assume that there are two clutters located in the same field as the target with transmit angles $\{44.5°, 45.5°\}$. Note that the closer the clutters are to the target, the greater their impact on the SCNR will be. Hence, we only consider the case when clutters are in the same field as the target with the greatest impact. For the NF clutters, their distance from the Tx is 7 m, this distance is 40 m for the FF clutters.

A. SINR Effect

In Fig. 3, the optimized beampatterns for different values of the communications SINR are presented. The scenarios include NFS-FFC, FFS-NFC, NF ISAC and FF ISAC. In NF ISAC, both CUs and target are in NF, while in FF ISAC both CUs and target are in FF. One sees that in both Fig. 3(a) and Fig. 3(b), when the CU SINR increases, or higher

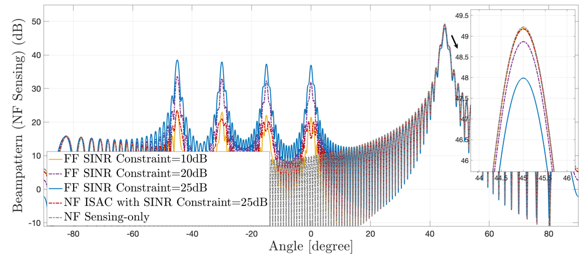

(a) NFS-FFC and NF ISAC

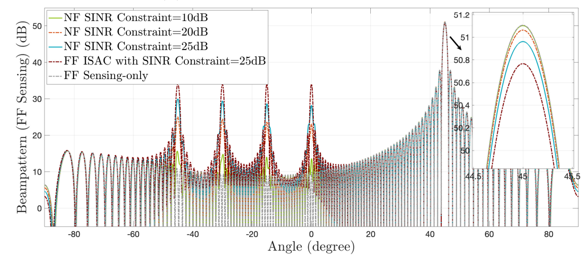

(b) FFS-NFC and FF ISAC

Fig. 3: Transmit beampattern with SINR Constraint=$10, 20, 25$ dB

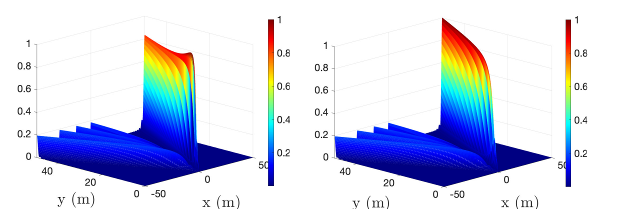

(a) NFS-FFC with NF model (b) NFS-FFC with FF model

Fig. 4: Normalized beampattern of NFS-FFC with NF and FF models.

communications rates are required, the sensing beampattern gain decreases. The shapes of the beampatterns and the main beam width of the beampatterns are approximately the same for all SINRs and sensing only. As for the NF ISAC or FFS-NFC, the NF CUs have lower beampatterns than the FF CUs in FF ISAC or NFS-FFC with the same SINR constraints, respectively. This is because, to achieve the same SINR, the FF CUs in FF ISAC and NFS-FFC need more power than the NF CUs in NF ISAC and FFS-NFC. This shows our proposed scheme also applies to FF only and NF only scenarios, but with different performances. The results above mean that the NF/FF communications can use the FF/NF sensing signals to realise the communications function without compromising the sensing performance too much. However, the sensing only case achieves the highest beam gain. The sidelobes in the beampatterns are due to signals transmitted to the CUs.

B. Normalized Beampattern

In Fig. 4, the normalized beampatterns using NFS-FFC for different propagation models are presented when CU SINR constraint is 20 dB. The angle-range 3D figure provides a clearer view. In Fig. 4(a), by applying the actual NF model, the optimized beam correctly focuses on the target coordinate $(10\text{m}, 45°)$, while in Fig. 4(b), by applying the mismatched FF model, the energy focuses only on the target angle.

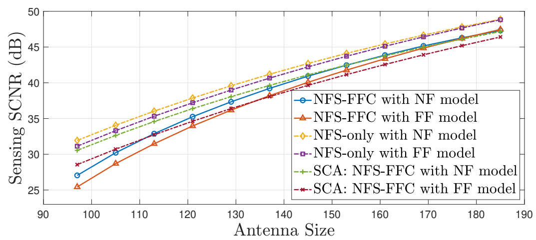

Fig. 5: The sensing SCNR of NFS with different antenna sizes

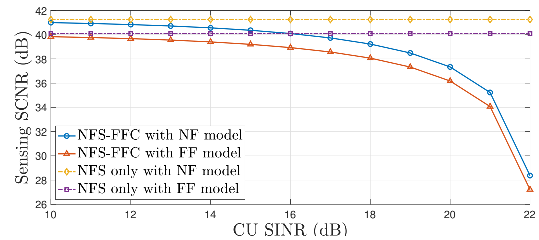

Fig. 6: The sensing SCNR of NFS with NF and FF models versus CU SINR

C. SCNR Versus Antenna Size and CU SINR

In this subsection, in addition to the proposed BF in (16), as in Fig. 4, the successive convex approximation (SCA)-based BF with sum rate (SR) constraint in [4] is added. 'NFS-FFC with NF model' refers to (20) assuming NF target, 'NFS-FFC with FF model' refers to (20) assuming FF target. 'NFS-only' refers to the corresponding results without ISAC. 'SCA' refers to the corresponding results using [4]. Fig. 5 shows the sensing performance for different propagation models as the number of antenna increases. The number of antennas ranges from 97 to 185 so that the target remains in the near field according to the effective Rayleigh distance, as this number changes the size of array and therefore NF region. In both NFS-only, NFS-FFC, and SCA-based NFS-FFC (SCA) scenarios, the sensing performance improves with the number of antennas. Note that, as the number of antennas increases, the sensing SCNR difference between schemes using NF model and schemes using FF model decreases. This is because for the NF clutters, the interference energy focuses on the clutter location, while for the FF clutters, the interference energy only focuses on the clutter angle. This makes the interference from NF clutters to increase more than that from FF clutters, as the number of antennas increases, or the NF clutters have larger interference to degrade the corresponding SCNR more to reduce the SCNR difference. Also, the SCA has worse performance than the proposed beamforming in most cases, except when the antenna size is less than 130 for FF, in which case its user fairness is poorer. Fig. 6 shows the sensing performance for different propagation models as the CU SINR increases. In NFS-only scenarios, the SCNR is unaffected by CUs and remains flat as CU SINR increases. In NFS-FFC scenarios, the sensing SCNR decreases as CU SINR requirements increase.

In both Fig. 5 and Fig. 6, the optimized SCNR with NF model is larger than the optimized SCNR with FF model for NFS only and NFS-FFC scenarios. This is expected, because the distance parameter r in the NF model makes the transmit energy focuses on the target location, and hence the leakage of the transmit energy to the clutters is suppressed. Previous works using optimization based on the FF model can only focus the energy on the target angle. Thus, using conventional FF-designed BF in the mixed field results in performance loss, and BF designed for mixed-field is necessary.

V. Conclusion

In this work, we have designed BF for mixed near- and far-field ISAC systems based on bi-static settings. Numerical results show that one cannot use conventional BF designs optimized for FF as BF for mixed field, as this incurs performance loss. The performance tradeoff has shown that the sensing SCNR increases with the decrease of CU SINR or rate requirements. In addition, both sensing and communications performances improve with increasing antenna size.

References

[1] F. Liu, Y. Cui, C. Masouros, J. Xu, T. X. Han, Y. C. Eldar, and S. Buzzi, "Integrated sensing and communications: Toward dual-functional wireless networks for 6g and beyond," *IEEE Journal on Selected Areas in Communications*, vol. 40, no. 6, pp. 1728–1767, 2022.

[2] H. Lu, Y. Zeng, C. You, Y. Han, J. Zhang, Z. Wang, Z. Dong, S. Jin, C.-X. Wang, T. Jiang *et al.*, "A tutorial on near-field xl-mimo communications towards 6g," *arXiv preprint arXiv:2310.11044*, 2023.

[3] J. Cong, C. You, J. Li, L. Chen, B. Zheng, Y. Liu, W. Wu, Y. Gong, S. Jin, and R. Zhang, "Near-field integrated sensing and communication: Opportunities and challenges," *arXiv preprint arXiv:2310.01342*, 2023.

[4] L. Chen, Z. Wang, Y. Du, Y. Chen, and F. R. Yu, "Generalized transceiver beamforming for DFRC with MIMO radar and MU-MIMO communication," *IEEE Journal on Selected Areas in Communications*, vol. 40, no. 6, pp. 1795–1808, 2022.

[5] Z. Ren, Y. Peng, X. Song, Y. Fang, L. Qiu, L. Liu, D. W. K. Ng, and J. Xu, "Fundamental CRB-rate tradeoff in multi-antenna ISAC systems with information multicasting and multi-target sensing," *IEEE Transactions on Wireless Communications*, pp. 1–1, 2023.

[6] B. Guo, J. Liang, G. Wang, B. Tang, and H. C. So, "Bistatic MIMO DFRC system waveform design via fractional programming," *IEEE Transactions on Signal Processing*, vol. 71, pp. 1952–1967, 2023.

[7] R. Li, Z. Xiao, and Y. Zeng, "Towards seamless sensing coverage for cellular multi-static integrated sensing and communication," *IEEE Transactions on Wireless Communications*, pp. 1–1, 2023.

[8] Z. Wang, X. Mu, and Y. Liu, "Near-field integrated sensing and communications," *IEEE Communications Letters*, vol. 27, no. 8, pp. 2048–2052, 2023.

[9] K. Qu, S. Guo, N. Saeed, and J. Ye, "Near-field integrated sensing and communication: Performance analysis and beamforming design," *IEEE Open Journal of the Communications Society*, vol. 5, pp. 6353–6366, 2024.

[10] Y. Zhang, C. You, L. Chen, and B. Zheng, "Mixed near- and far-field communications for extremely large-scale array: An interference perspective," *IEEE Communications Letters*, vol. 27, no. 9, pp. 2496–2500, 2023.

[11] J. He, L. Li, T. Shu, and T.-K. Truong, "Mixed near-field and far-field source localization based on exact spatial propagation geometry," *IEEE Transactions on Vehicular Technology*, vol. 70, no. 4, pp. 3540–3551, 2021.

[12] M. Cui, L. Dai, Z. Wang, S. Zhou, and N. Ge, "Near-field rainbow: Wideband beam training for XL-MIMO," *IEEE Transactions on Wireless Communications*, vol. 22, no. 6, pp. 3899–3912, 2023.

[13] T. S. Rappaport, *Wireless communications: Principles and practice, 2/E*. Pearson Education India, 2010.

[14] B. Tang, J. Tang, Y. Zhang, and Z. Zheng, "Maximum likelihood estimation of dod and doa for bistatic mimo radar," *Signal Processing*, vol. 93, no. 5, pp. 1349–1357, 2013.

[15] Z.-q. Luo, W.-k. Ma, A. M.-c. So, Y. Ye, and S. Zhang, "Semidefinite relaxation of quadratic optimization problems," *IEEE Signal Processing Magazine*, vol. 27, no. 3, pp. 20–34, 2010.

[16] M. Grant and S. Boyd, "CVX: Matlab software for disciplined convex programming, version 2.1," http://cvxr.com/cvx, Mar. 2014.